Supporting Information for:

NanoLuc Complementation Reporter Optimized for Accurate Measurement of Protein Interactions in Cells

Andrew S. Dixon[†,§], Marie K. Schwinn[†], Mary P. Hall[†], Kris Zimmerman[†], Paul Otto[†], Thomas H. Lubben[†], Braeden L. Butler[†], Brock F. Binkowski[†], Thomas Machleidt[†], Thomas A. Kirkland[‡], Monika G. Wood[†], Christopher T. Eggers[†], Lance P. Encell*[,†], and Keith V. Wood[†]

[†]Promega Corporation, Madison, Wisconsin 53711 United States
[‡]Promega Biosciences Incorporated, San Luis Obispo, California 93401 United States
[§]Present address: Department of Pharmaceutics and Pharmaceutical Chemistry, University of Utah, Salt Lake City, Utah 84112 United States

**To whom correspondence should be addressed*:
2800 Woods Hollow Road, Madison, Wisconsin 53711 United States
Tel.: 608-274-1181; e-mail: lance.encell@promega.com

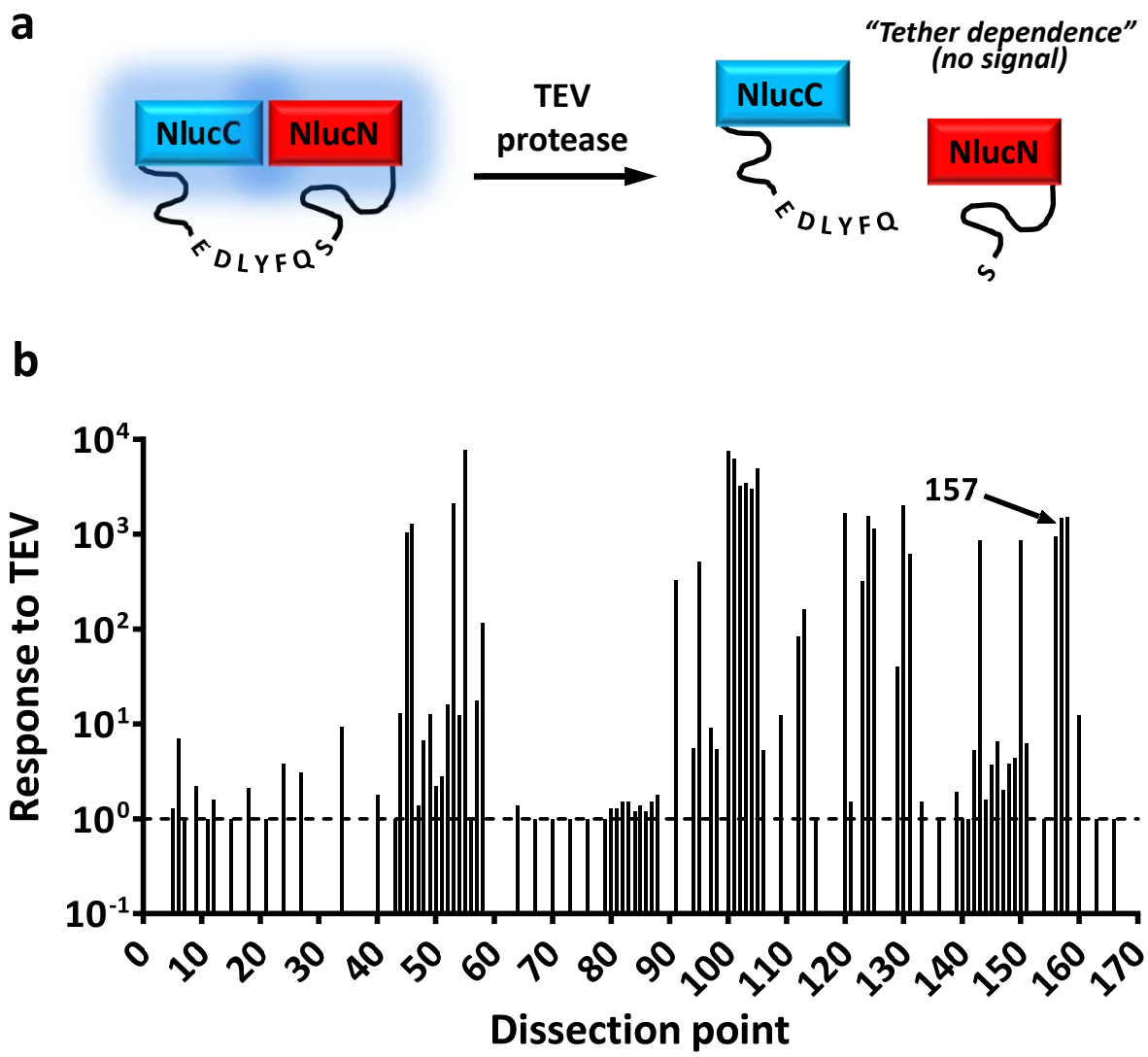

Supporting Figure s1. Defining a dissection point in NanoLuc (Nluc). (a) Schematic of the assay used to screen for dissection points in Nluc resulting in fragments with low intrinsic binding affinity. Of 170 possible circularly permuted (CP) variants, 90 (~50%) were constructed comprising fragments of Nluc tethered by a 33-amino acid cleavable linker (NlucN = native N-terminal fragment; NlucC = native C-terminal fragment; EDLYFQS = TEV protease recognition site). Luminescence was measured in the absence and presence of TEV protease, where loss of signal following proteolytic cleavage indicated "tether dependence," i.e., fragments (presumably with low intrinsic binding affinity) requiring a proximity constraint imposed by the tether to maintain productive luminescence. (b) Response to TEV treatment for the 90 variants. Dashed line represents variants that did not respond to TEV (i.e., (-)TEV/(+)TEV = 1). CP-157 was the preferred variant moving forward because of high tether dependence and the fact that one of the fragments was a 13-amino acid peptide.

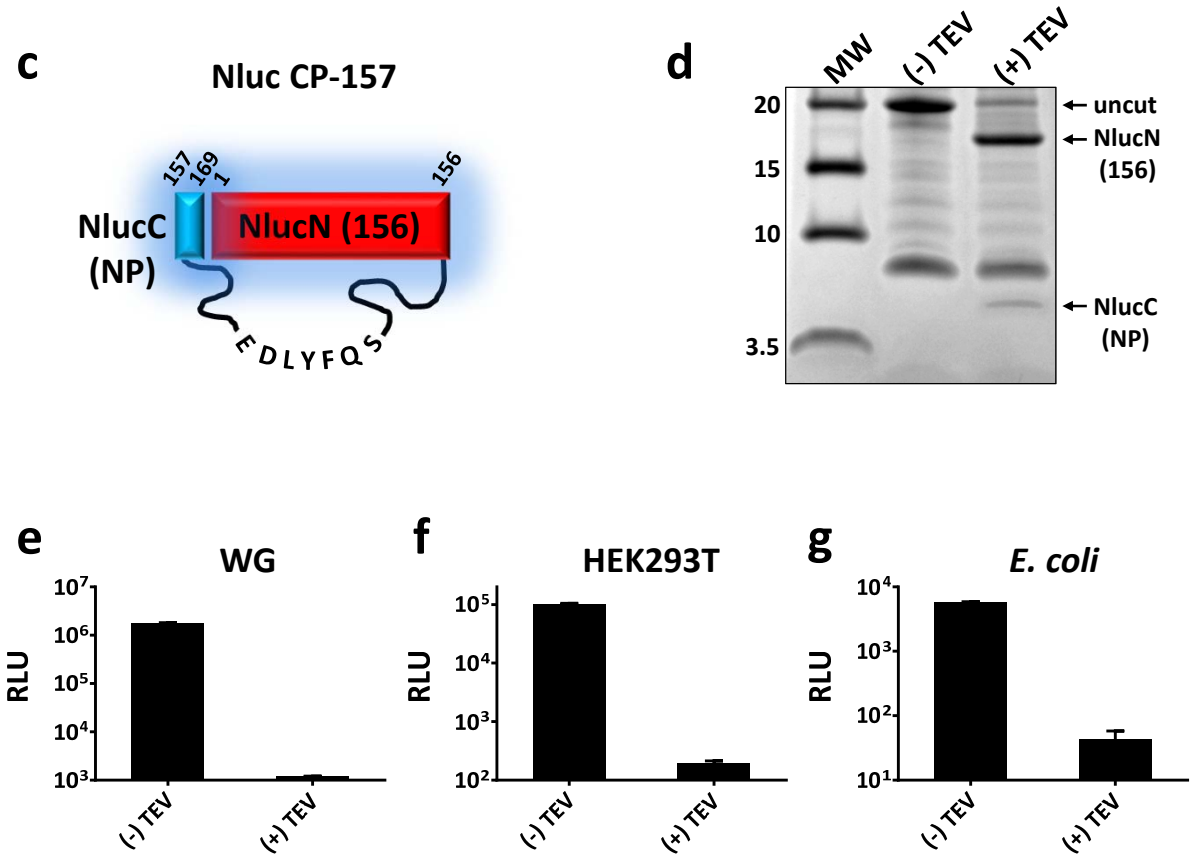

Supporting Figure s1 (cont'd). Defining a dissection point in NanoLuc (Nluc). (c) Nluc CP-157 schematic showing the native 13 C-terminal residues (NlucC, NP) relocated to the N-terminus and the larger, native N-terminal fragment (NlucN, 156) relocated to the C-terminus. (d) SDS-PAGE image of undiluted bacterial lysates containing overexpressed Nluc CP-157 that were either untreated (-) or treated (+) with TEV protease. The image indicates TEV proteolysis was efficient and produced fragments of the appropriate size. (e–g) Loss of relative luminescence (RLU) upon treatment with TEV protease for CP-157 in the context of Wheat Germ (WG) lysates (panel e), HEK293T lysates (panel f), and *E. coli* KRX lysates (panel g). n = 3, variability displayed as S.D. for panels e-g.

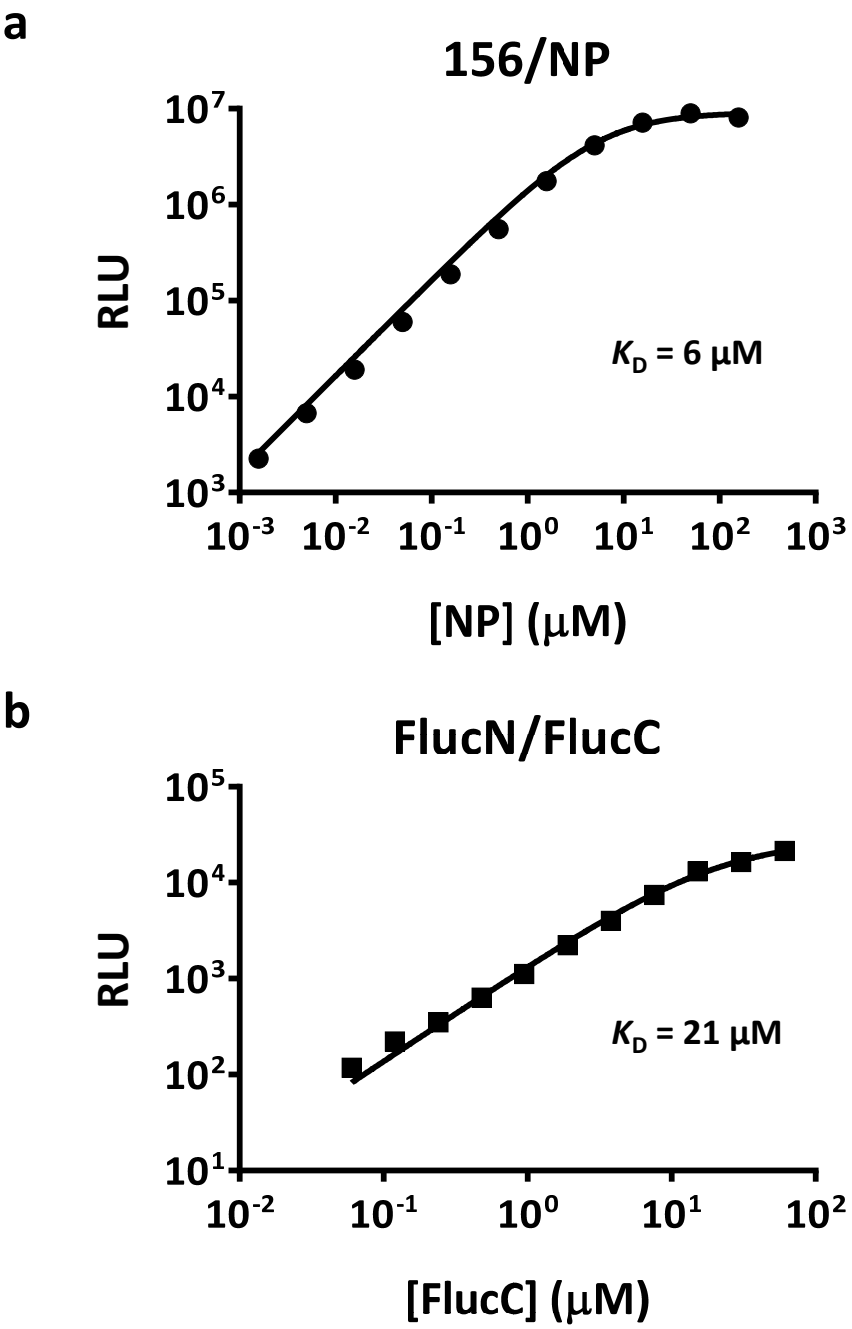

Supporting Figure s2. Binding affinity between 156 and NP and between split Fluc fragments. (a) Titration of 156 with NP. (b) Titration of FlucC with FlucN (FlucN = native residues 4–398; FlucC = native residues 394–544). Data was fit to the model for one site specific binding, and resulting fit was used to determine apparent K_D for each binding pair (displayed on plots). Data shown on double log plot to highlight linearity at sub-saturation. n = 3, variability displayed as S.D. for both panels.

a

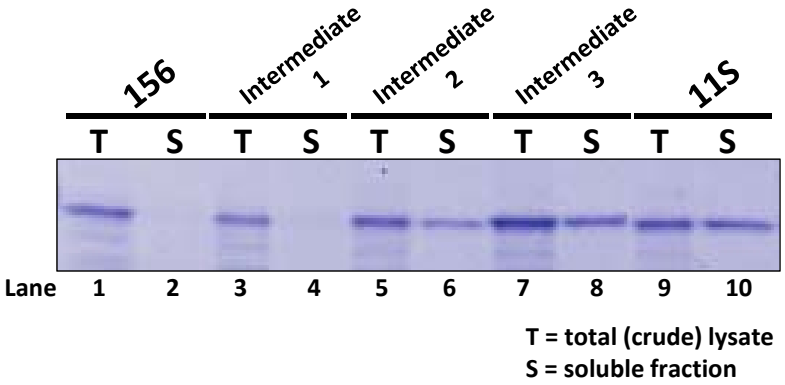

b

```
          1       8          18          28          38          48          58
156     MVFTLEDFVG DWRQTAGYNL DQVLEQGGVS SLFQNLGVSV TPIQRIVLSG ENGLKIDIHV
11S                  E   A                  L   A           R     A

                68          78          88          98         108         118
156     IIPYEGLSGD QMGQIEKIFK VVYPVDDHHF KVILHYGTLV IDGVTPNMID YFGRPYEGIA
11S              A   A   EV                  P               LN

              128         138         148      156
156     VFDGKKITVT GTLWNGNKII DERLINPDGS LLFRVTIN
11S                           T     M       S
```

Supporting Figure s3. Summary of sequence optimization. (a) Expression levels and solubility in *E. coli* lysates resulting from the optimization process. SDS-PAGE indicating the amount of both total and soluble protein produced by 156 (lanes 1, 2), a series of three intermediate variants (lanes 3–8), and the final evolved variant, 11S (lanes 9, 10). Although 156 was essentially insoluble, almost complete solubility was achieved for 11S through sequence optimization. (b) Amino acid sequence of 156 aligned with the substitutions in 11S. Substitutions in 156 resulting from the original development of Nluc are shown in red. 11S substitutions are shown in blue (note that Phe in the third position is referred to as residue #1). Substitutions to alanine were identified through rational mutagenesis. See Supporting Table s1 for additional sequence details.

Supporting Table s1. Amino acid substitutions in 11S (corresponding residues for Nluc and the source of Nluc, *Oplophorus gracilirostris* small catalytic luciferase subunit (Oluc-19), are shown for reference.)

Position	Oluc-19	Nluc	**11S**
11	Q	R	**E**
15	G	G	**A**
31	F	F	**L**
35	G	G	**A**
46	L	L	**R**
51	G	G	**A**
67	G	G	**A**
71	G	G	**A**
75	M	K	**E**
76	I	I	**V**
93	H	H	**P**
107	I	I	**L**
108	D	D	**N**
144	N	N	**T**
149	L	L	**M**
157	G	G	**S***

*Insertion of an extra C-terminal residue, not a true Gly>Ser substitution. The starting sequence for optimization contained a C-terminal Val as part of a restriction site (Pme1). The residue was found to be frequently mutated in improved variants, and ultimately Ser was discovered to provide the best expression of luminescence activity.

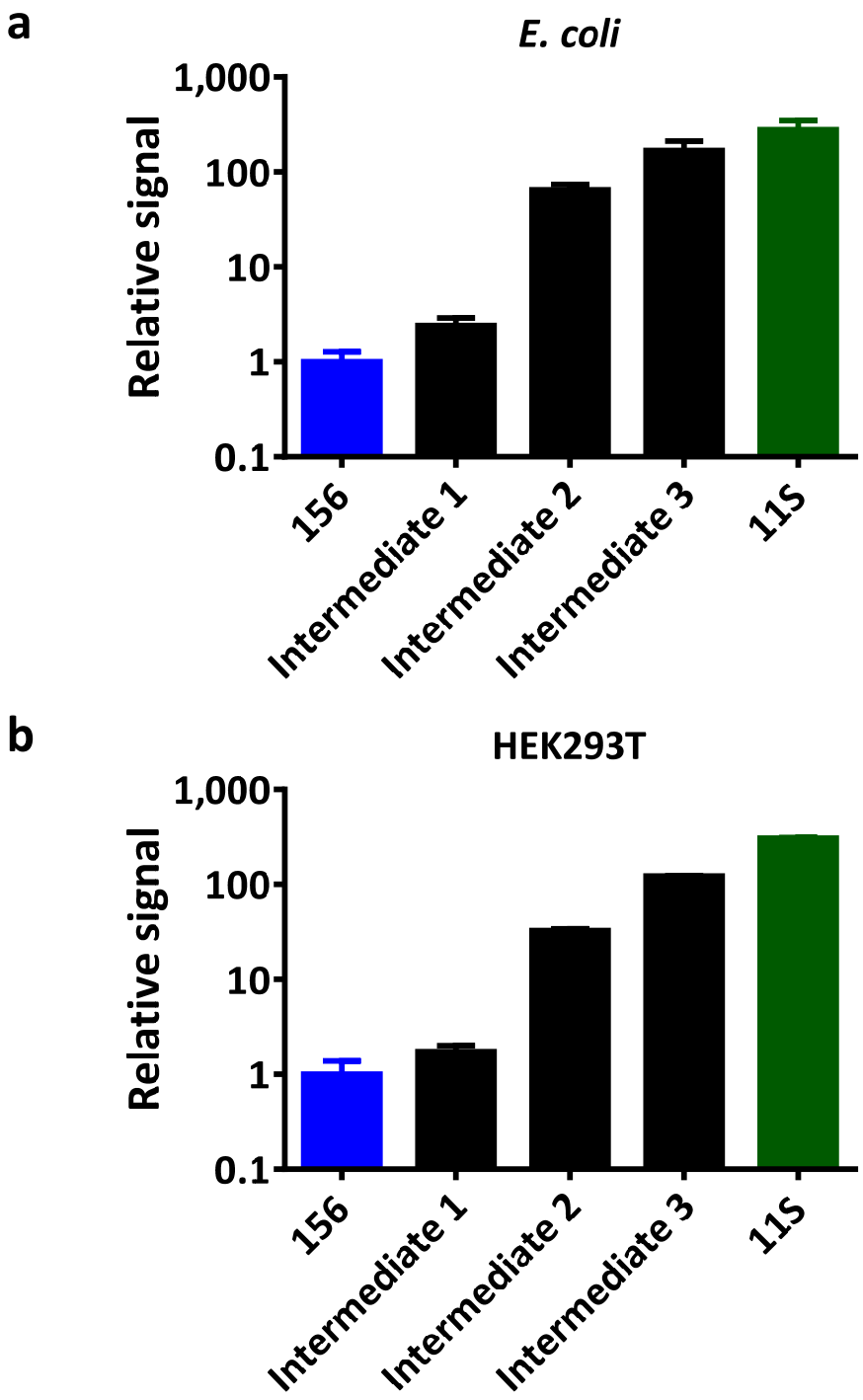

Supporting Figure s4. Relative luminescence improvements in *E. coli* KRX and HEK293T resulting from the optimization process. Relative signal in the presence of saturating NP for 156, a series of three intermediate variants, and the final evolved variant, 11S. RLUs normalized to 156; n = 3, variability displayed as S.D. for both panels. These results indicate a pattern of improvement consistent with the optimized expression shown in Supporting Figure s3. These results also demonstrate that the improvements selected in *E. coli* (panel a) translate to similar improvements in mammalian cells (panel b).

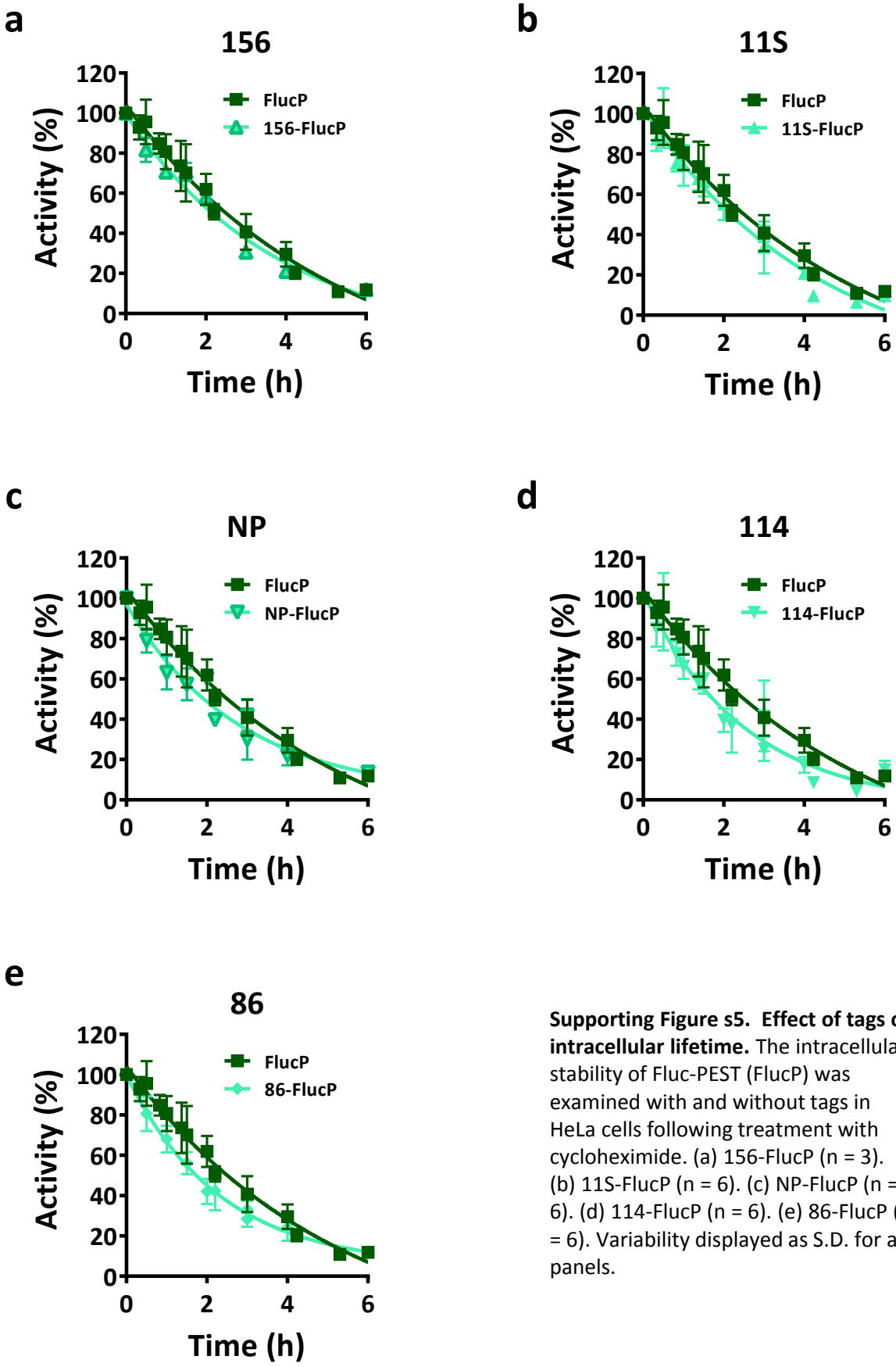

Supporting Figure s5. Effect of tags on intracellular lifetime. The intracellular stability of Fluc-PEST (FlucP) was examined with and without tags in HeLa cells following treatment with cycloheximide. (a) 156-FlucP (n = 3). (b) 11S-FlucP (n = 6). (c) NP-FlucP (n = 6). (d) 114-FlucP (n = 6). (e) 86-FlucP (n = 6). Variability displayed as S.D. for all panels.

Supporting Table s2. Peptide numeric name, amino acid sequence (aligned to Nluc positions 157–169), and the equilibrium dissociation constant (K_D) for each (based on binding to 11S). Amino acids shown in red represent deviations from NP (boxed).

Peptide	157	158	159	160	161	162	163	164	165	166	167	168	169	K_D (M)*
86	-	V	S	G	W	R	L	F	K	K	I	S	-	**0.7×10^{-9}**
78	N	V	S	G	W	R	L	F	K	K	I	S	N	**3.4×10^{-9}**
79	N	V	T	G	Y	R	L	F	K	K	I	S	N	**8.5×10^{-9}**
99	-	V	T	G	Y	R	L	F	E	K	I	S	-	**1.8×10^{-7}**
128	-	V	T	G	Y	R	L	F	E	K	I	L	-	**2.8×10^{-7}**
NP	G	V	T	G	W	R	L	C	E	R	I	L	A	**0.9×10^{-6}**
104	-	V	E	G	Y	R	L	F	E	K	I	S	-	**1.3×10^{-6}**
101	-	V	T	G	Y	R	L	F	E	K	E	S	-	**2.5×10^{-6}**
114	-	V	T	G	Y	R	L	F	E	E	I	L	-	**1.9×10^{-4}**

*Peptides listed in order of decreasing affinity. Variation in sequence and size was found to modulate binding affinity by greater than 5 orders of magnitude (~1 nM to ~200 µM).

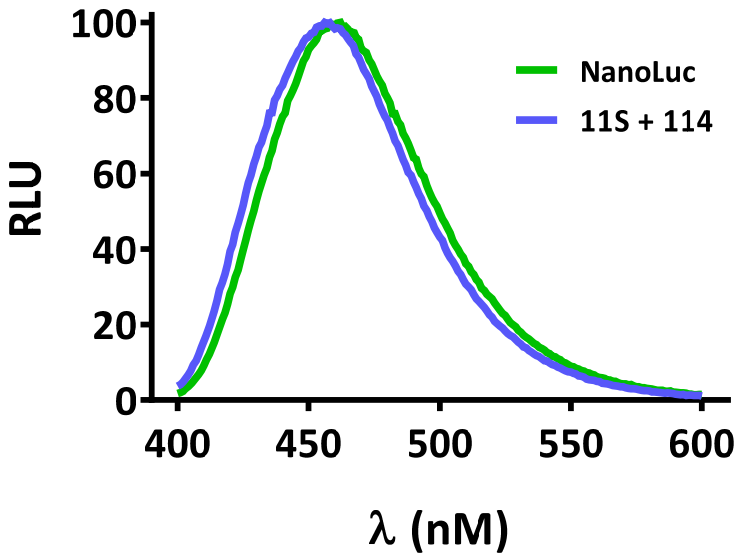

Supporting Figure s6. Emission spectra for Nluc versus 11S + 114. Spectral profiles for NanoLuc and 11S + 114 (substrate = furimazine). Emission peaks: Nluc (461 nm), 11S + 114 (457 nm). Data represent averages of six replicates.

Supporting Table s3. Peptide numeric name, amino acid sequence (aligned to Nluc positions 158–168). (see Supporting Figure s7)

Peptide	158	159	160	161	162	163	164	165	166	167	168
86	V	S	G	W	R	L	F	K	K	I	S
219		S	G	W	R	L	F	K	K	I	S
206			G	W	R	L	F	K	K	I	S
235				W	R	L	F	K	K	I	S
214					R	L	F	K	K	I	S
229	V	S	G	W	R	L	F	K	K	I	
228	V	S	G	W	R	L	F	K	K		
227	V	S	G	W	R	L	F	K			
226	V	S	G	W	R	L	F				
225	V	S	G	W	R	L					
224	V	S	G	W	R						
87		S	G	W	R	L	F	K	K	I	
97		S	G	W	R	L	F	K	K		
218		S	G	W	R	L	F	K			
217		S	G	W	R	L	F				
216		S	G	W	R	L					
215		S	G	W	R						
205			G	W	R	L	F	K	K	I	
161			G	W	R	L	F	K	K		
188			G	W	R	L	F	K			
204			G	W	R	L	F				
184			G	W	R	L					
203			G	W	R						
234				W	R	L	F	K	K	I	
199				W	R	L	F	K	K		
192				W	R	L	F	K			
186				W	R	L	F				
233				W	R	L					
232				W	R						

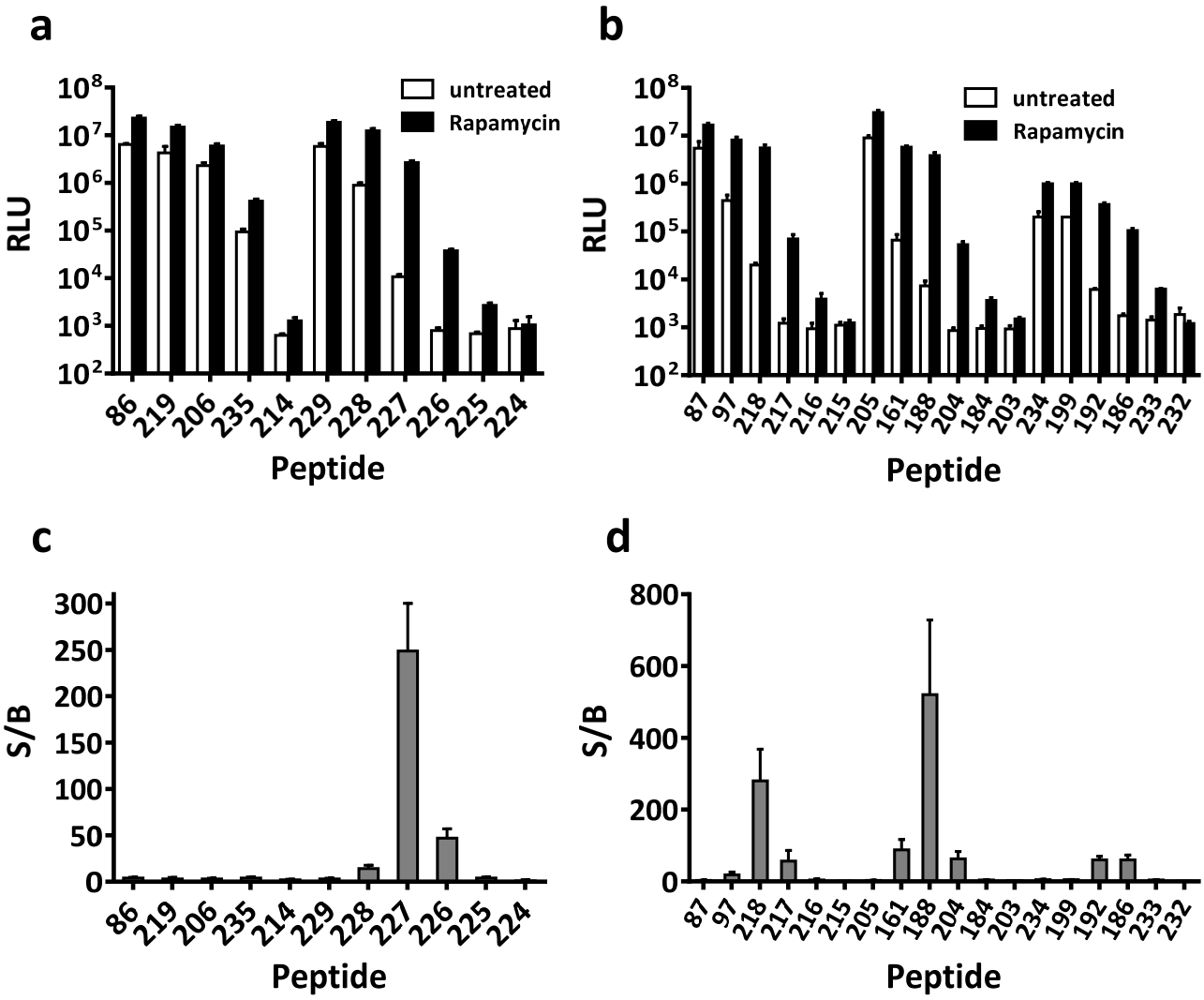

Supporting Figure s7. Identification of the minimal peptide required for binary complementation with 11S. (a,b) HEK293T cells were transfected with FRB-11S and FKBP fused (via a 15 Gly-Ser linker; see METHODS section) to different peptide variants (0.1 ng total DNA per well of 96-well plate). Samples were treated with 30 nM rapamycin for 2 h and measured for luminescence. (c,d) Conversion of the data in panels a, b to signal over background (S/B). n = 4, variability displayed as S.D. for all panels.

Supporting Table s4. Linker sequences. (see Supporting Figure s8).

Linker	Sequence														
15	G	G	S	G	G	G	G	S	G	G	S	S	S	G	G
10	G	G	G	G	S	G	G	G	G	S					
8			G	G	S	G	G	G	G	S					
6					S	G	G	G	G	S					
5						G	G	G	G	S					
4							G	G	G	S					
3								G	G	S					
2									G	S					
1										S					
0										S					

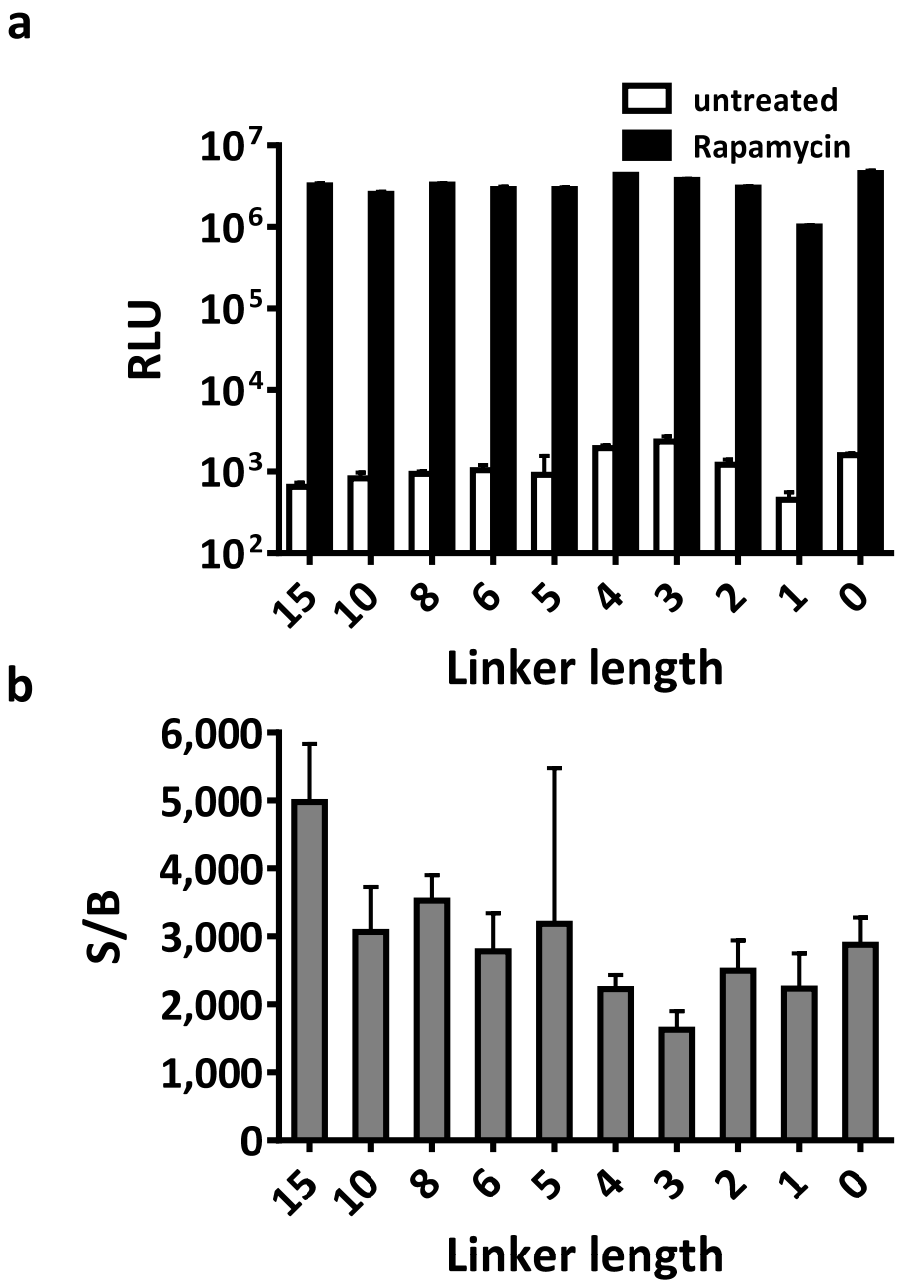

Supporting Figure s8. Identification of the minimal linker required for binary complementation. (a) HEK293T cells were transfected with FRB-11S and variants of FKBP-114 (0.1 ng total DNA per well of a 96-well plate). FRB-11S contained the standard 15-amino acid linker, (see METHODS) while the FKBP-114 linker was varied as indicated. Cells were treated with 30 nM rapamycin for 2 h and measured for luminescence. (b) Conversion of the data in panel a to signal over background (S/B). n = 4, variability displayed as S.D. for both panels.

Supporting Table s5. Peptide numeric name, amino acid sequence (aligned to Nluc positions 158–168). (see Supporting Figure s9)

Peptide	158	159	160	161	162	163	164	165	166	167	168
114	V	T	G	Y	R	L	F	E	E	I	L
143	V	T	G	Y	R	L	F	E	E	I	
231	V	T	G	Y	R	L	F	E	E		
230	V	T	G	Y	R	L	F	E			
223		T	G	Y	R	L	F	E	E	I	L
222		T	G	Y	R	L	F	E	E	I	
221		T	G	Y	R	L	F	E	E		
220		T	G	Y	R	L	F	E			
209			G	Y	R	L	F	E	E	I	L
208			G	Y	R	L	F	E	E	I	
207			G	Y	R	L	F	E	E		
177			G	Y	R	L	F	E			
239				Y	R	L	F	E	E	I	L
238				Y	R	L	F	E	E	I	
237				Y	R	L	F	E	E		
236				Y	R	L	F	E			
86	V	S	G	W	R	L	F	K	K	I	S
227	V	S	G	W	R	L	F	K			
218		S	G	W	R	L	F	K			
188			G	W	R	L	F	K			
192				W	R	L	F	K			

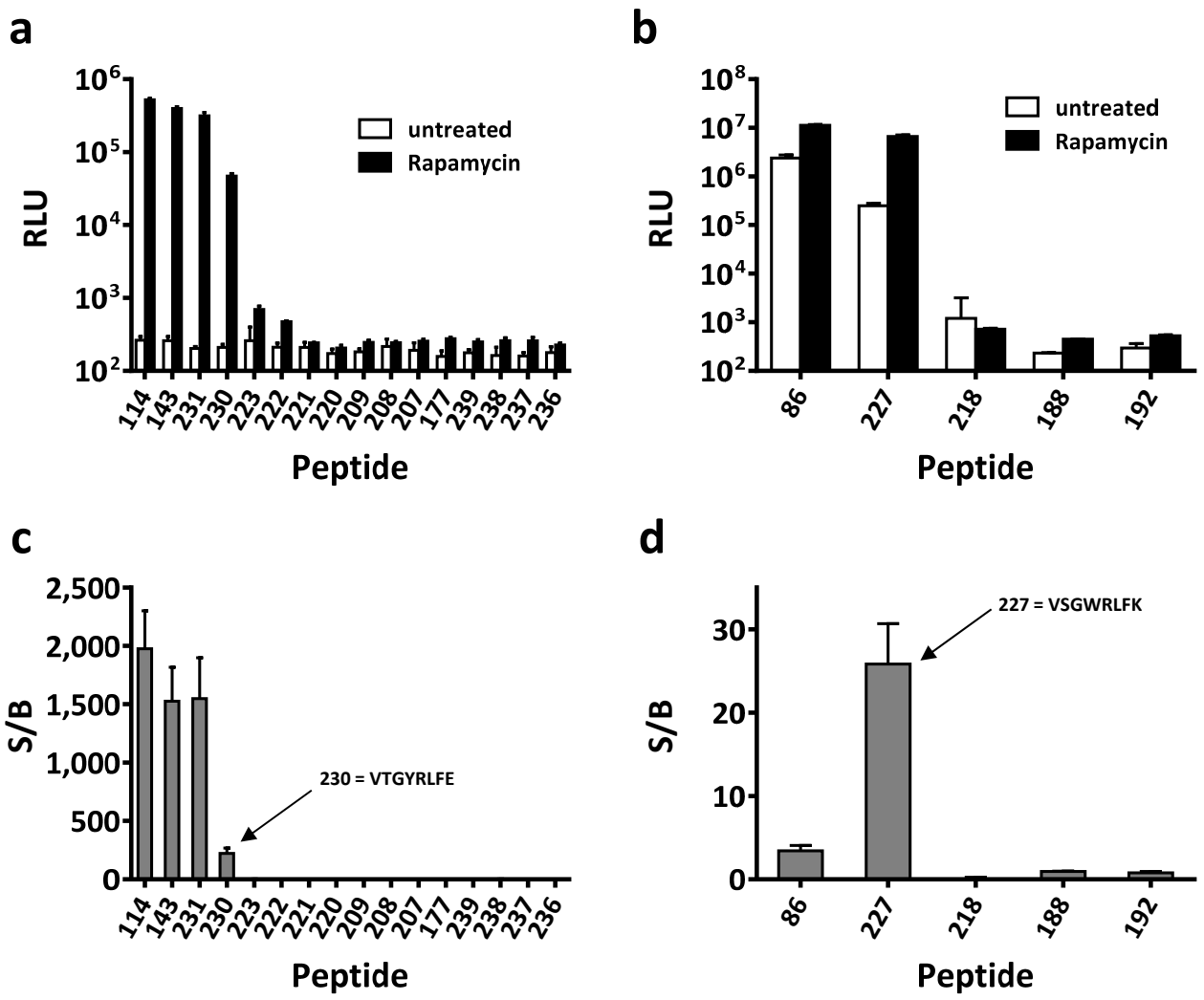

Supporting Figure s9. Identification of the minimal sequence required for binary complementation without linker. (a,b) HEK293T cells were transfected with FRB-11S and FKBP fused directly (no linker) to different peptides (0.1 ng per well of a 96-well plate). Cells were treated with 30 nM rapamycin for 2 h and measured for luminescence. (c,d) Conversion of the data in panels a, b to signal over background (S/B). n = 4, variability displayed as S.D. for all panels. Note the 8-mer peptides, 230 (panel c) and 227 (panel d) were the smallest functional sequences.

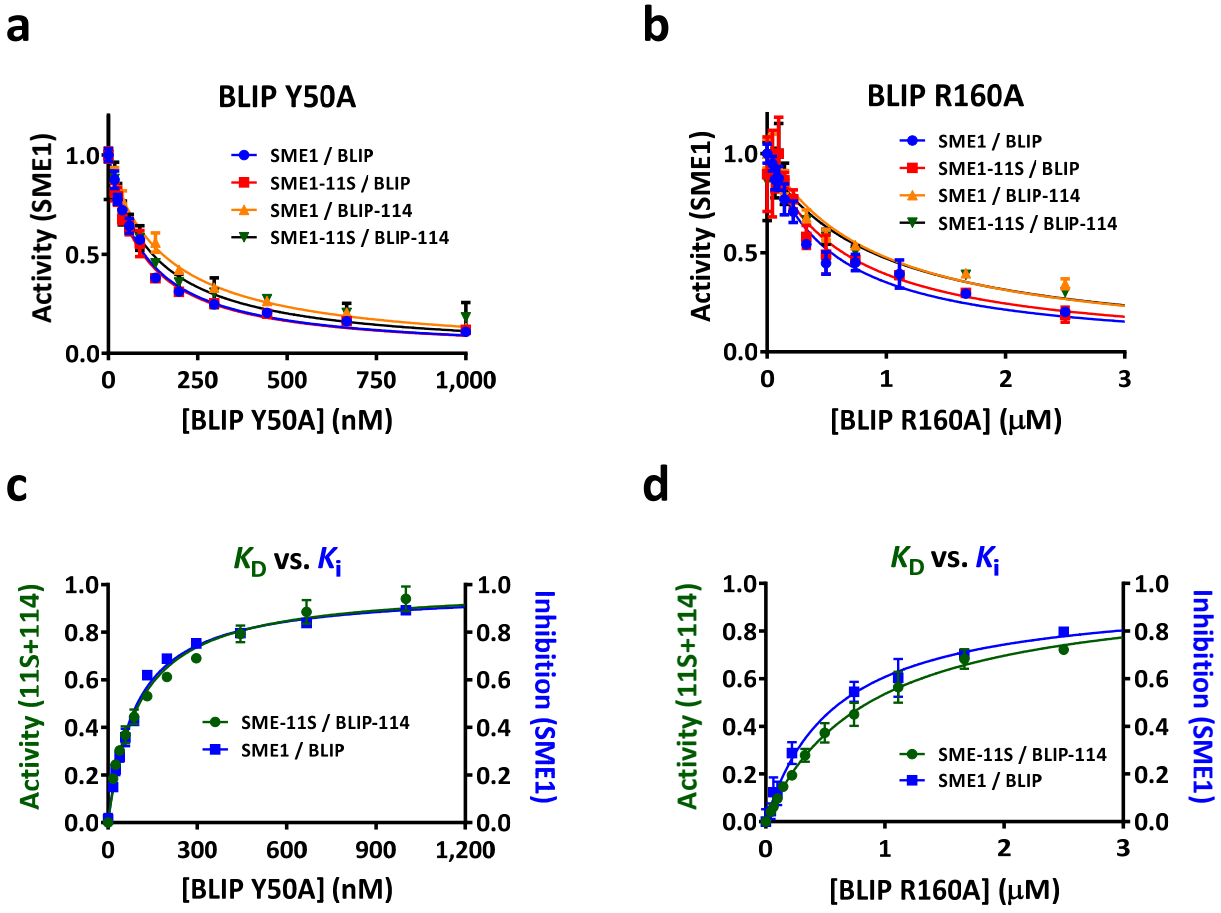

Supporting Figure s10. Binding between BLIP and SME. (a,b) Activity of SME1 in presence of increasing concentrations of BLIP mutants Y50A and R160A. Data normalized to signal in the absence of BLIP. (c,d) Binding between SME1 and BLIP Y50A or BLIP R160A as measured through SME activity and NanoBiT luminescence. n = 3, variability displayed as S.D. for all panels.

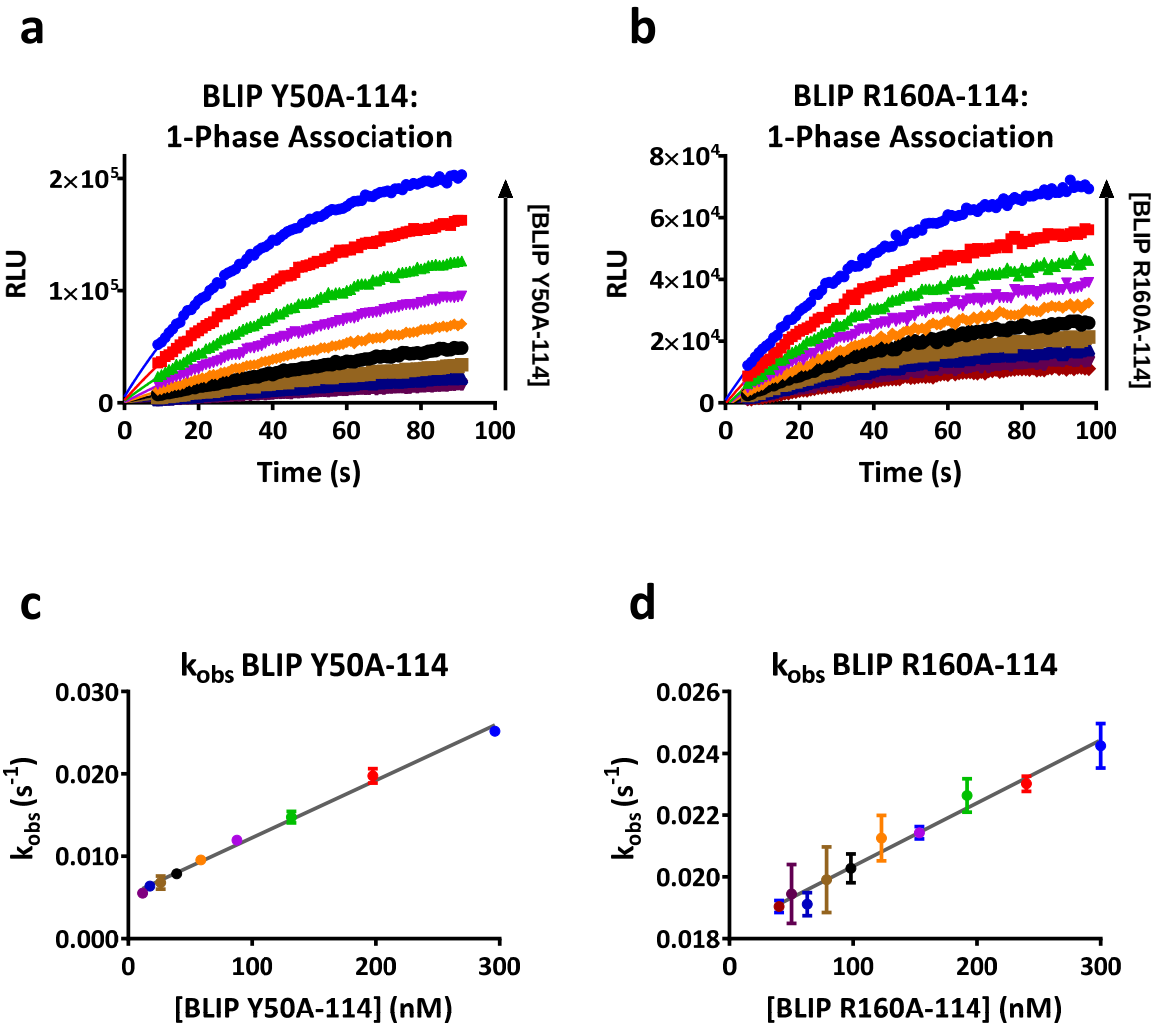

Supporting Figure s11. Determination of association and dissociation rate constants using NanoBiT. (a) Time course for generation of luminescence following addition of BLIP Y50A-114. (b) Time course for generation of luminescence following addition of BLIP R160A-114. (c) Observed rate constant determined by fitting time-dependent increase in luminescence to one-phase association for various concentrations of BLIP Y50A-114. (d) Observed rate constant determined by fitting time-dependent increase in luminescence to one-phase association for various concentrations of BLIP R160A-114. n = 3, variability displayed as S.D. for all panels.

a

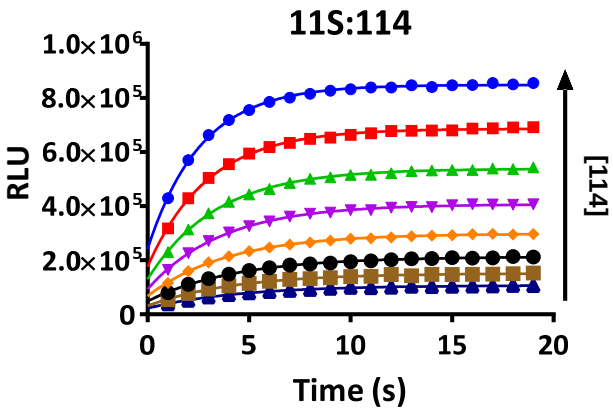

b

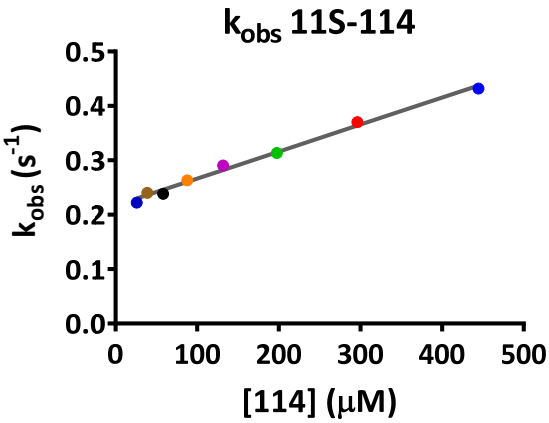

c

k_{on} (μM^{-1} s^{-1})	5.0 ± 0.2 x 10^{-4}
k_{off} (s^{-1})	2.2 ± 0.0 x 10^{-1}
K_D (μM)	440

Supporting Figure s12. Binding kinetics between 11S and 114. (a) Time course for luminescence following injection of 114. (b) Observed rate constants for each concentration of 114. (c) Association and dissociation rate constants determined from the line fit to the plot of the observed rate constants versus concentration; Equilibrium dissociation constant (K_D) as determined from k_{off}/k_{on}.

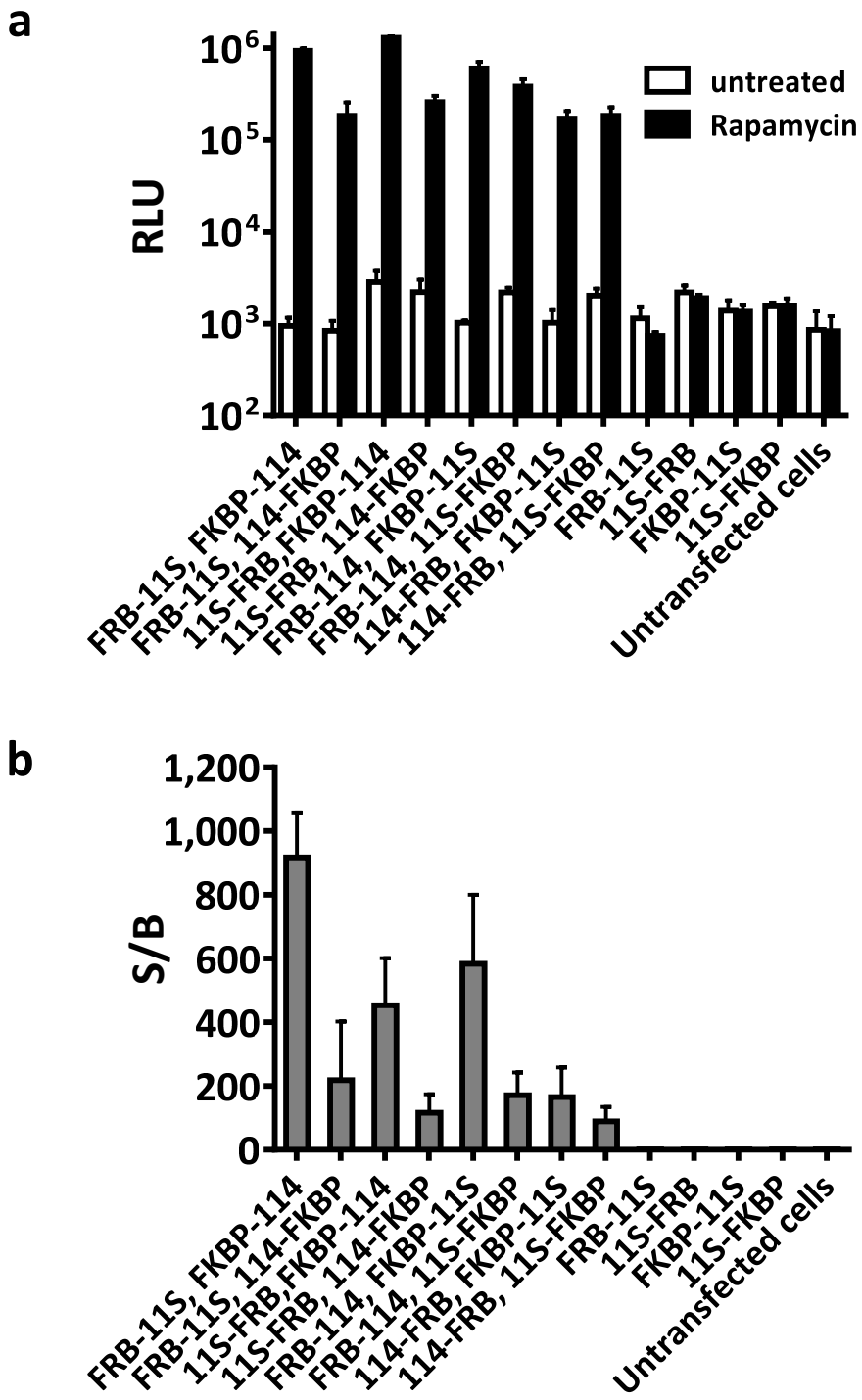

Supporting Figure s13. Identification of the optimal configuration of 11S and 114 for detecting the rapamycin-inducible interaction between FRB and FKBP. (a) HEK293T cells were transfected with all 8 possible configurations of 11S and 114 fused to FRB and FKBP, treated with 30 nM rapamycin for 2 h, and measured for luminescence. (b) Conversion of the data in panel a to signal over background (S/B). This analysis identified FRB-11S and FKBP-114 as the optimal configuration to be used for further experiments. n = 4, variability displayed as S.D. for both panels.

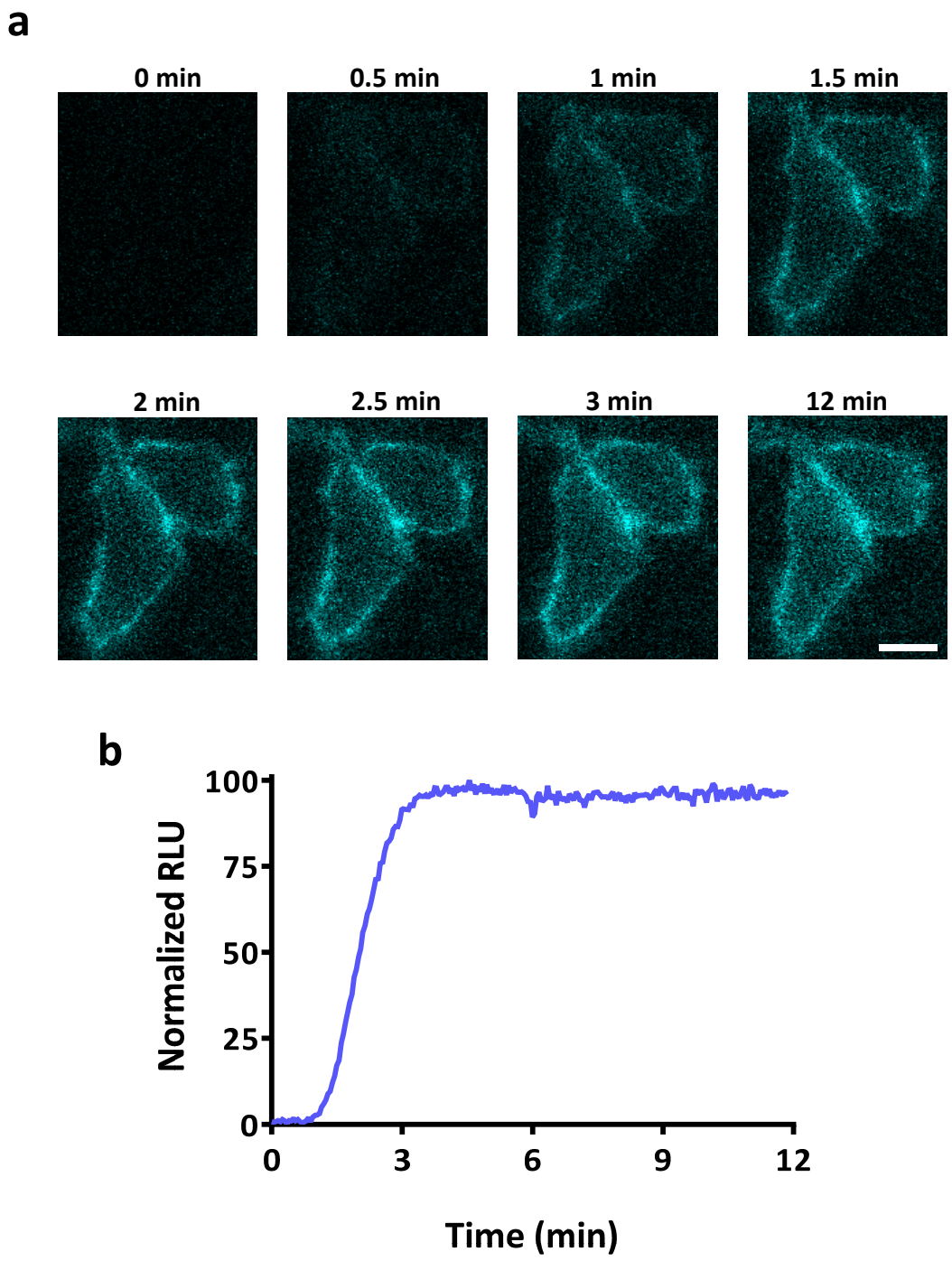

Supporting Figure s14. Bioluminescence imaging of ligand-induced interactions between NanoBiT fusions. (a) HeLa cells expressing AVPR2-114 and 11S-ARRB2 were treated with 1 µM AVP, and images were acquired every 2 s for 12 min (EM gain = 600). Panels show pseudo-colored images of the NanoBiT interaction at indicated time points following stimulation with AVP (scale bar = 10 µm). (b) Analysis of kinetics of AVP-induced interaction between AVPR2-114 and 11S-ARRB2. Shown is the kinetic trace obtained from a single representative cell.

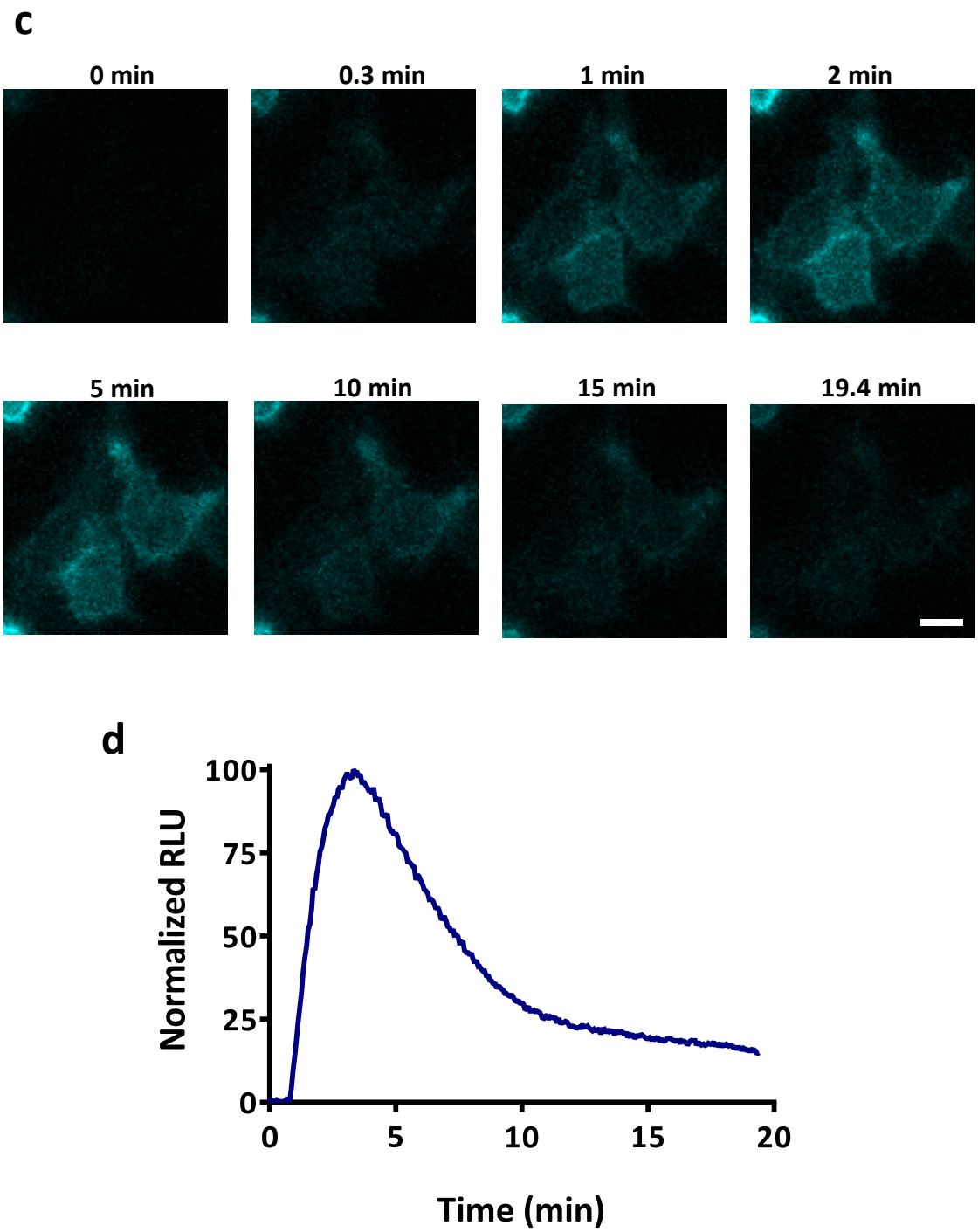

Supporting Figure s14 (cont'd). Bioluminescence imaging of ligand-induced interactions between NanoBiT fusions. c) HeLa cells expressing ADRB2-11S and 114-ARRB2 were treated with 100 µM isoproterenol, and images were acquired every 4 s for 20 min using (EM gain = 400). Panels show pseudocolored images of the NanoBiT interaction at indicated times following stimulation with isoproterenol (scale bar = 10 µm). (d) Kinetics of isoprotenerol induced interaction between ADBR2-11S/114-ARRB2 obtained from a single representative cell.

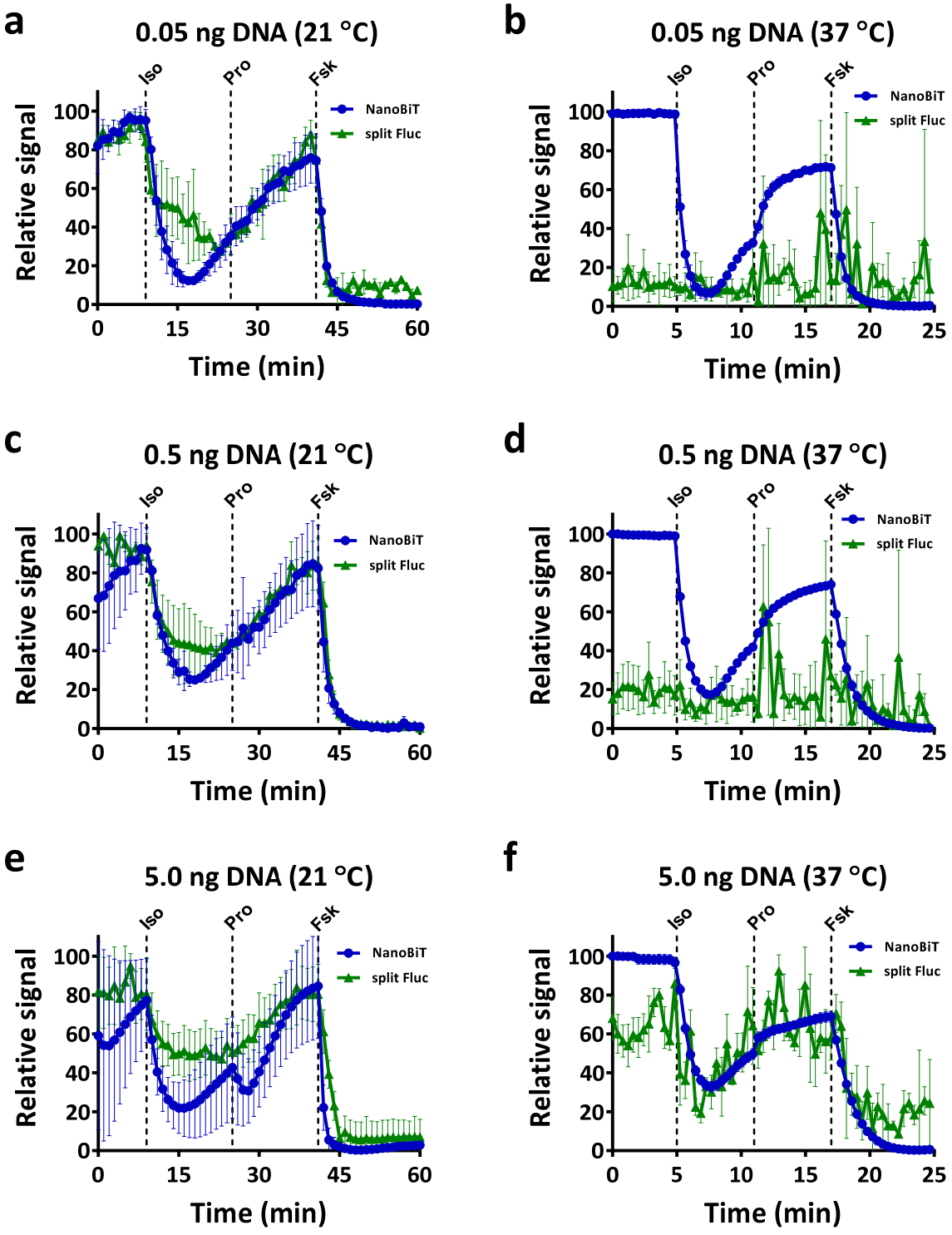

Supplemental Figure s15. Comparing NanoBiT to split Fluc for monitoring protein kinase A dynamics at different temperatures. HEK293T cells were transiently transfected with varying amounts of plasmid DNA (equal mass ratio) to monitor the PRKACA/PRKAR2A interaction with NanoBiT (panels a, c, e) and split Fluc (panels b, d, f). Vertical dashed lines represent addition of 10 µM isoproterenol (Iso), 10 µM propranolol (Pro), and 10 µM forskolin (Fsk). Additional details on experimental conditions can be found in the main text METHODS section (Intracellular luminescence/Kinetic measurements). n = 3, variability displayed as S.D. for all panels.

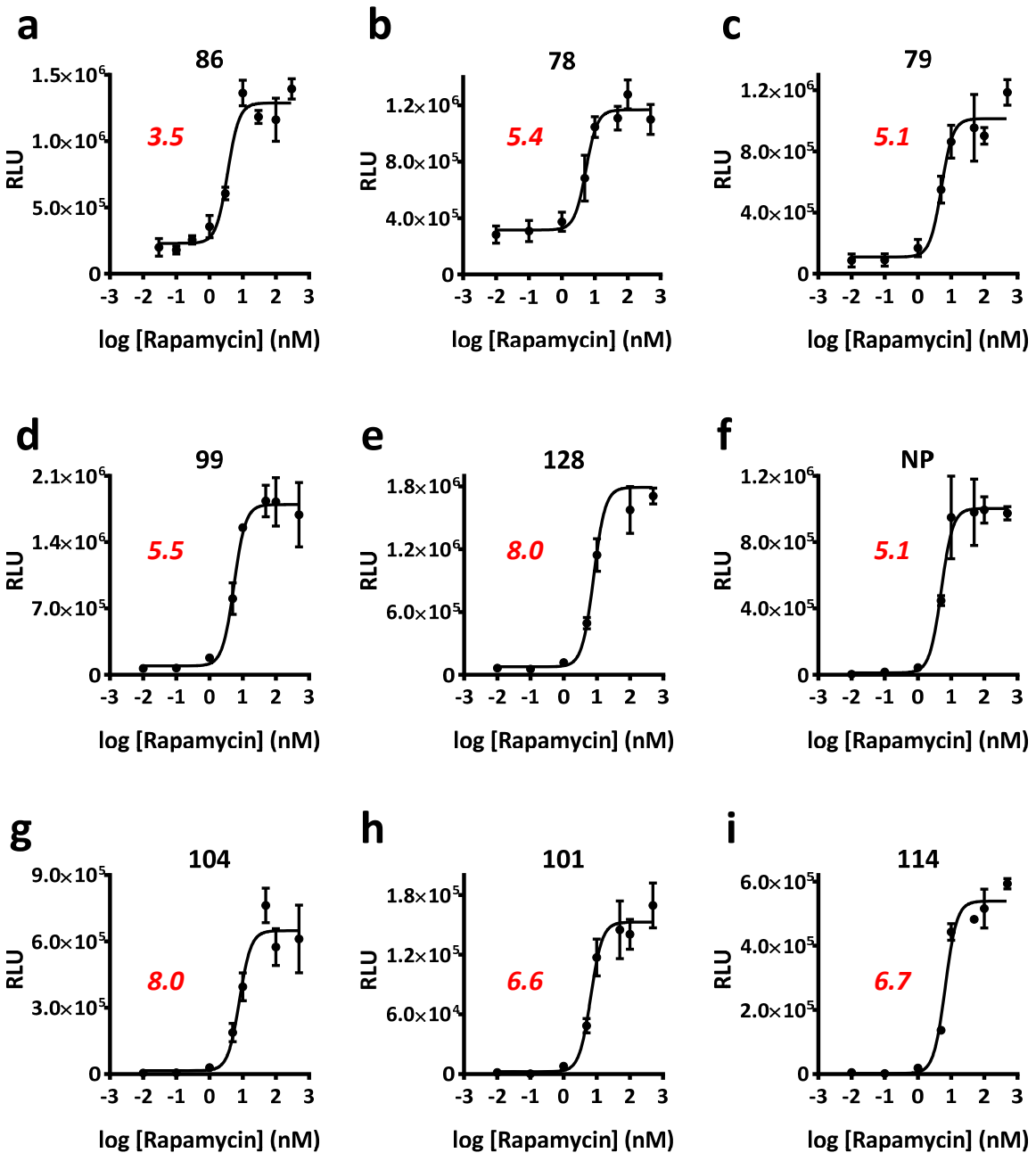

Supporting Figure s16. Rapamycin EC_{50} determinations for FRB/FKBP interaction using 11S coupled with different peptides. The FRB/FKBP interaction was induced using variable rapamycin in HEK293T cells co-transfected with 50 pg/well FRB-11S and 50 pg/well FKBP fused to the different peptides. (a) Peptide 86 (b) Peptide 78 (c) Peptide 79 (d) Peptide 99 (e) Peptide 128 (f) Peptide NP (g) Peptide 104 (h) Peptide 101 (i) Peptide 114. Each data set was fit to a sigmoidal dose-response model (Hill slope 2.5) for the three part binding between FRB/FKBP/rapamycin according to Banaszynski *et al.* (2005) (see main text REFERENCES section). EC_{50} values (nM) shown in red for each plot. n = 4, variability displayed as S.D. for all panels.

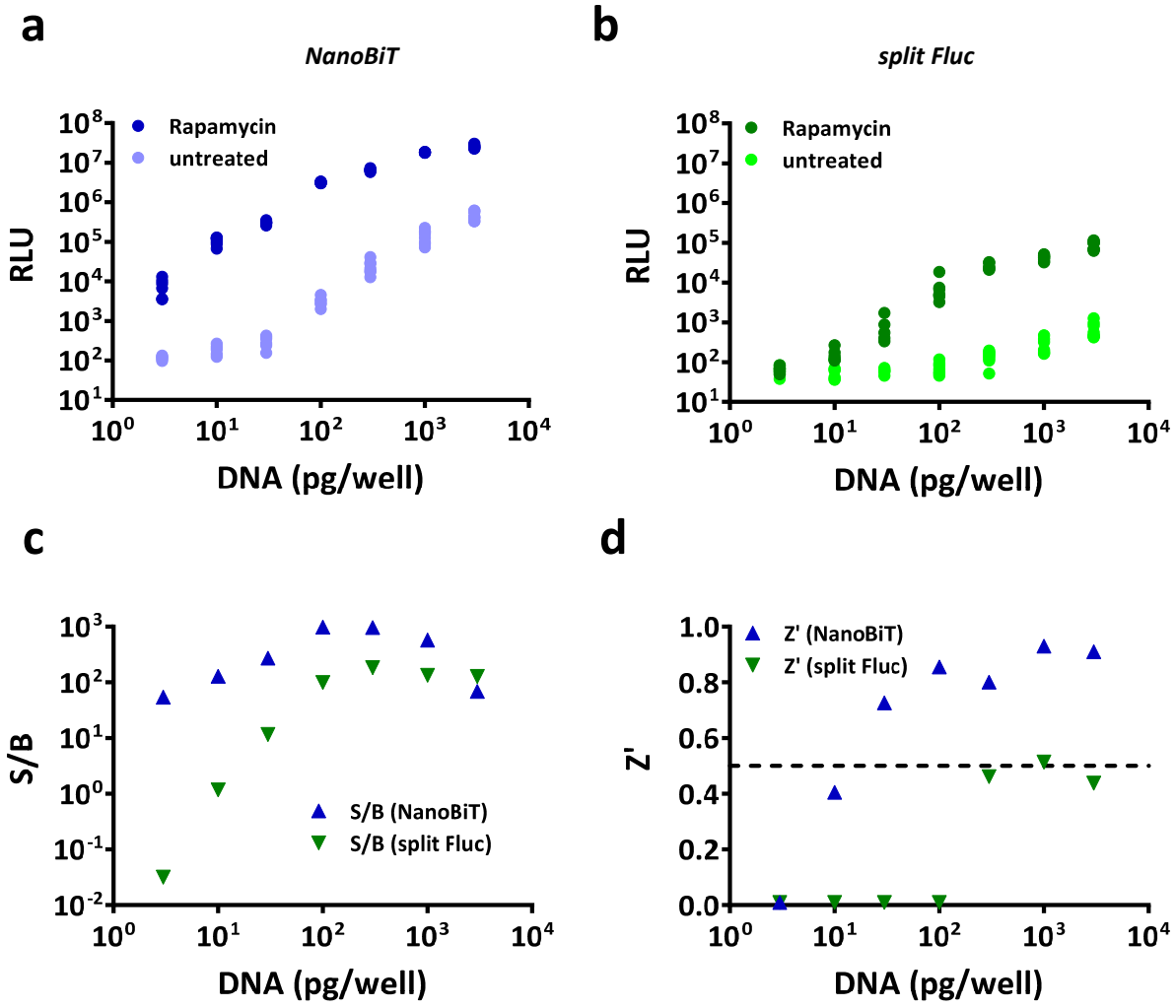

Supporting Figure s17. Comparing NanoBiT and split Fluc (optimal configurations) for assay performance in the context of rapamycin-inducible FRB/FKBP. (a,b) HEK293T cells transfected with the indicated amounts of DNA per well (96-well plate) were treated (+/- 30 nM rapamycin, 2 h) and measured for luminescence. Variability is shown for 8 independent samples for each DNA concentration across two different source plates. RLUs for each of 8 samples are plotted for each DNA concentration along with the mean and S.E.M. (c) Signal over background (S/B) for data from panels a, b. (d) Z' of data from panels a, b; calculated using the formula: $Z' = 1-3*(\sigma_{signal} + \sigma_{background})/(x_{signal} - x_{background})$. NanoBiT was as much as 1,000-fold brighter. Additionally, it showed higher precision, provided greater sensitivity (S/B), and was more robust (Z'). Generally acceptable Z' values are ≥0.5 (horizontal dashed line).

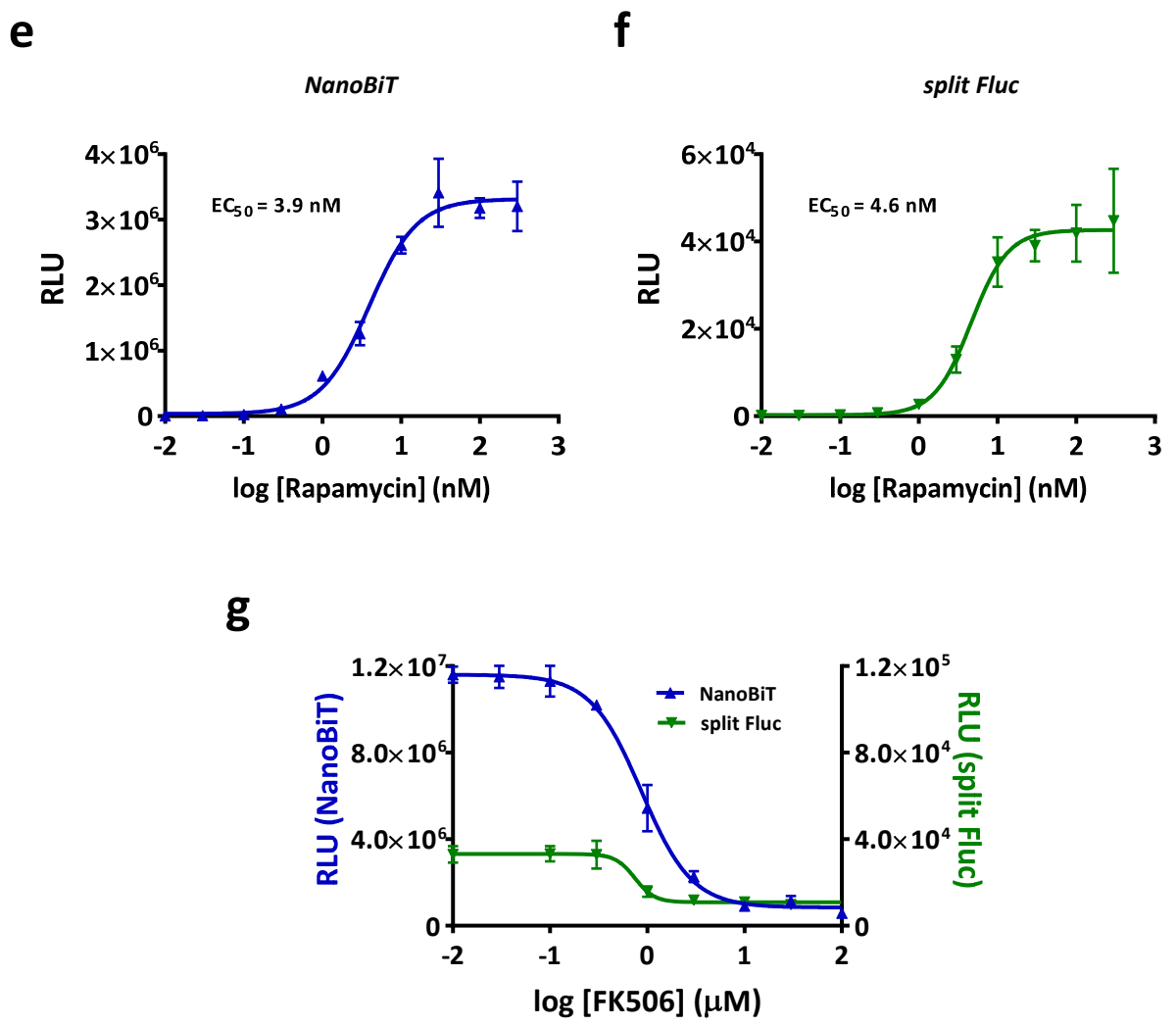

Supporting Figure s17 (cont'd). Comparing NanoBiT and split Fluc (optimal configurations) for assay performance in the context of rapamycin-inducible FRB/FKBP. Rapamycin dose response curves were generated using HEK293T cells co-transfected with optimal concentrations of FRB-11S and FKBP-114 (100 pg/well, panel e) or FlucN-FRB and FKBP-FlucC (1 ng/well, panel f). Each point represents the average RLU of 8 samples across at least two plates, and variability is represented by S.D. for both panels. Both systems generated accurate EC_{50} values for rapamycin. (g) Reversibility of NanoBiT and split Fluc was assessed using the competitive inhibitor, FK506. Cells were transfected with 100 pg NanoBiT or 1 ng split Fluc DNA per well (96-well assay plate) and then pre-incubated with 30 nM rapamycin for 2 h, followed by a 4 h treatment with FK506. n = 3, variability displayed as S.D. Both systems were effective at monitoring drug-induced reversibility of the FRB/FKBP complex, however in addition to a higher signal, NanoBiT showed superior dynamic response to FK506. In summary, these results suggest that assessing an assay strictly on the ability to precisely measure EC_{50}values or reversibility may not necessary reflect the quantitative capabilities of the assay.

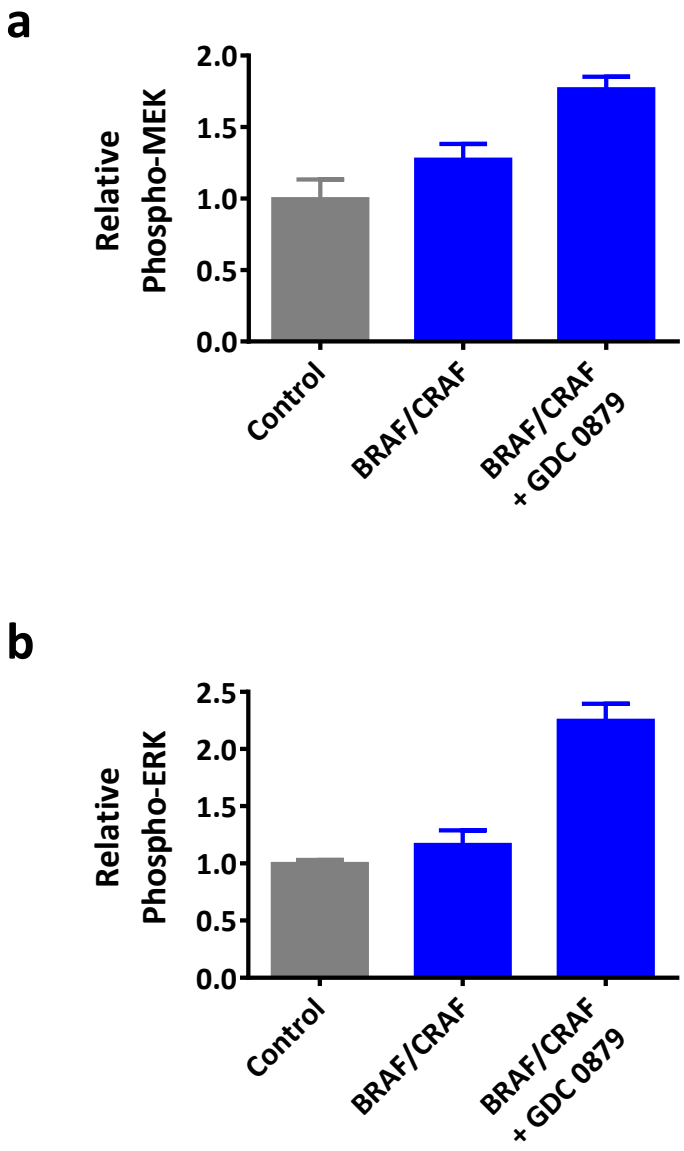

Supporting Figure s18. Biological activity of cells expressing NanoBiT BRAF and CRAF fusions. (a,b) Phosphorylation of MEK1/2 and ERK1/2 measured by ELISA. HCT116 cells transiently transfected with BRAF-11S/CRAF-114 were serum-starved and treated with 3 µM GDC 0879 for 5 h. These plots show MEK1/2 and ERK1/2 phosphorylation levels relative to untransfected (control) cells. n = 6, variability displayed as S.D. for both panels.

SUPPORTING METHODS

Reagents and Cell Culture. Unless otherwise stated, all chemicals were from Sigma Aldrich, Flexi® Vectors and *E. coli* strains were from Promega, cell lines were from American Type Culture Collection, and cell culture reagents were from Thermo Fisher Scientific. HEK293T (CRL-3216) and HeLa (CCL-2) cells were maintained in Dulbecco's Modified Eagle Medium (DMEM)/10% fetal bovine serum at 37 °C with 5% CO_2. HCT116 (CCL-247) were maintained in McCoy's 5A (Modified) Medium/10% fetal bovine serum. Transfections were carried out using FuGENE® HD Transfection Reagent (Promega) at a lipid:DNA ratio of 3:1. In these transfections, pGEM®3Z carrier DNA (Promega) was used to achieve total DNA levels of 50 ng per well of 96-well plate. Phenol red-free Opti-MEM®I was used as the buffered cell culture medium for luminescence measurements. The FACE™ MEK1/2 and FACE™ ERK1/2 assays (Active Motif) were used to measure MEK and ERK phosphorylation in the BRAF/CRAF assays.

Preparation of Extracts and Lysates for Screening Circularly Permuted (CP) Variants. To prepare wheat germ extracts, variants (pF4Ag) were expressed (T7 promoter) using the TNT® T7 Coupled Wheat Germ Extract System (Promega) and diluted 1:100 in PBS (pH 7.2) containing 0.1% gelatin. To prepare mammalian lysates, HEK293T cells transiently expressing (CMV promoter) CP variants (pF4Ag) were lysed with Passive Lysis Buffer (Promega) and then diluted 1:10 in PBS (pH 7.2) containing 0.1% gelatin. To prepare bacterial lysates, CP variants (pF4Ag) were overexpressed (T7 promoter) in Single Step (KRX) Competent Cells, and individual colonies were picked and grown overnight at 30 °C. The cultures were diluted 1:100 in LB broth + ampicillin, grown to an OD_{595} of 0.5 at 37 °C, and induced at 25 °C for 18 h in the presence of 0.2% rhamnose. Cells were lysed by freeze/thaw, diluted 1:10 in PBS (pH 7.2), and then the soluble fraction was collected.

Preparation of Bacterial Lysates for Screening Directed Evolution Mutants. KRX *E. coli* library colonies (3,696) were grown in M9 minimal medium (1X M9-salts, 0.1 mM $CaCl_2$, 2 mM $MgSO_4$, 1 mM thiamine HCl, 1% (w/v) gelatin, 0.2% (v/v) glycerol, 100 μg/ml ampicillin) at 37 °C with shaking for 17–

20 h. The cultures were diluted 1:20 into fresh medium and grown for another 17–20 h at 37 °C. Expression was auto-induced at 25 °C for 17–20 h by diluting cultures 1:20 into medium containing 0.05% (w/v) glucose and 0.02% (w/v) rhamnose. Cultures were diluted 1:5 in lysis buffer (50 mM HEPES pH 7.5, 0.3X Passive Lysis Buffer, 6 U/ml RQ1 RNase-Free DNase (Promega)).

Protein Purification. 156, 11S, Nluc, and FlucC (Fluc residues 394-544) were expressed as HaloTag fusions from the pFN18K HaloTag® T7 Flexi® Vector and purified from KRX cells using HaloLink™ Resin (Promega).[1-3] FlucN (Fluc residues 4-398) was expressed as a HaloTag fusion from the pFN21K HaloTag® CMV Flexi® Vector and purified from HEK293T cells using HaloLink™ Resin according to a previously described method.[4] Concentrations were determined using the Pierce™ 660 nm Protein Assay (Thermo Fisher Scientific).

BLIP and SME1 genes were synthesized (Gene Dynamics, LLC) and sub-cloned (as non-fusions or fusions to NanoBiT components) into the pF1K T7 Flexi® Vector (Promega). Constructs were designed to encode the native BLIP/SME1 signal sequences and a 6xHis tag at the N-terminus of each protein as previously described.[5] NanoBiT sequences, i.e., 11S and 114, were introduced using gene splicing by overlap extension.[6] KRX cultures containing the expression vector were grown overnight at 37 °C and diluted 1:100 into LB + kanamycin. Following 3 h incubation at 37 °C, cells were induced with 0.2% rhamnose at 25 °C (SME1 and SME1-11S) or 16 °C (BLIPs and BLIP-114s) overnight. SME1 was purified using a Maxwell® 16 Polyhistidine Protein Purification Kit (Promega) on a Maxwell®16 Instrument (Promega). SME1-11S, BLIP, and BLIP-114 expression cultures were pelleted and sonicated in 20 mM Tris pH 8 containing 500 mM NaCl. Soluble lysate was applied to a HisTALON™ Superflow Cartridge (Clontech) and eluted with imidazole. BLIPs and BLIP-114s were dialyzed into 25 mM Tris at either pH 7.5 (BLIP R160A and BLIP-114) or pH 8 (BLIP WT and BLIP Y50A) containing 25 mM NaCl and further purified on a HiTrap Q Sepharose FF column (GE Healthcare). SME1 and SME1-11S concentrations were

determined by the Pierce™ 660 nm Protein Assay, and BLIP and BLIP-114 concentrations were determined by absorbance at 280 nm.

Split Fluc Affinity. Purified FlucN was diluted to 33 nM in assay buffer (50 mM Tris pH 8, 0.01% Prionex, 0.005% Tergitol®, 1 mM DTT, and 30 mM $MgSO_4$) and incubated with various concentrations of FlucC for 30 min at ambient temperature. ATP and D-luciferin in the same buffer were then added to final concentrations of 30 and 3 mM, respectively. Luminescence was monitored for 1 h, and the maximal signal at each FlucC concentration was fit (One site–specific binding) using GraphPad Prism 6, and the fits were subsequently used to determine K_D values.

Intracellular Stability of Fused Target Protein (FlucP reporter). 156, 11S, NP, 114 and 86 were fused to the N-terminus of FlucP[7] (P = PEST degradation sequence) in the pF4Ag CMV-D1 Flexi®Vector.[8] Transiently transfected HeLa cells were plated at a density of 1 x 10^4 cells/well and incubated overnight at 37 °C. Medium was exchanged with growth medium containing 0.4 mM cycloheximide or DMSO, and cells were incubated at 37 °C for the indicated time. The remaining FlucP signal was assayed by addition of ONE-Glo™ (Promega) and measured on a GloMax-Multi+ Detection System (Promega) after 3 min incubation. Cycloheximide-treated samples were normalized to DMSO-treated samples for each time point and data were fit using GraphPad Prism 6.

Western Blotting. For Western blotting of 156, 11S and Nluc, lysates were generated from HEK293T cells by repeated cycles of freeze/thaw. Proteins were separated by SDS-PAGE and transferred to PVDF membranes. Membranes were probed with either rabbit anti-Nluc polyclonal IgG (Promega) or rabbit anti-β-actin polyclonal IgG (Abcam) at 1:5,000 dilutions and then incubated with Goat Anti-Rabbit IgG-HRP secondary antibody (Promega). For all other Western blots, lysates were prepared using RIPA Buffer (Thermo Fisher Scientific) containing EDTA-Free Halt™ Protease Inhibitor Cocktail (Thermo Fisher Scientific). Membranes were incubated with rabbit polyclonal anti-FKBP (Abcam) at a dilution of 1:2,000 or rabbit polyclonal anti-FRB (Enzo Life Sciences) at a dilution of 1:500 followed by incubation with

peroxidase-conjugated AffiniPure Donkey Anti-Rabbit IgG secondary antibody (Jackson ImmunoResearch Laboratories) at a dilution of 1:5,000. Signals were detected using the ECL Western Blotting Substrate (Promega) in combination with the ImageQuant LAS 4000 digital imaging system (GE Healthcare).

Emission Spectra. Spectral resolution was carried out as previously described[9]. 100 pM Nluc or 100 pM 11S with 100 µM 114 were incubated in the presence of 10 µM furimazine (all dilutions made in OptiMEM+0.01% BSA) and spectra taken in 1 nm steps using a Tecan-M1000 reader. Averages were calculated from six replicates at each wavelength.

Expression Vectors Used in Live Cell Assays. cDNA of FKBP (NM_000801), FRB (amino acids 2019-2112 of MTOR, NM_004958), BRAF (NM_004333), CRAF (NM_002880), ARRB2 (NM_004313), AVPR2 (NM_000054), ADRB2 (NM_000024), PRKACA (NM_002730), and PRKAR2A (NM_004157) were obtained from Kazusa DNA Research Institute. Open reading frames were transferred to a pF5K-based Flexi® Vector (Promega) which resulted in NanoBiT fusions utilizing either the 15-amino acid linker GSSGGGGSGGGGSSG (FKBP, FRB, ARRB2, AVPR2, ADRB2, PRKACA, and PRKAR2A) or the 10-amino acid linker GGGGSGGGGS (BRAF and CRAF). cDNA (FKBP, FRB, PRKACA, and PRKAR2A) were also transferred to pF5K-based Flexi® Vectors expressing FlucN (1-398) or FlucC (394-544) fusions with the 10-amino acid linker. In studies comparing different peptide sequences, C-terminal FKBP peptide fusions were generated by inserting duplex oligonucleotide cassettes (Integrated DNA Technologies) into pF5K-based Flexi® Vectors containing the 10-amino acid linker.

Bioluminescence Imaging of Protein Interactions. All imaging experiments were performed using a LV200 Inverted Microscope Bioluminescence Imaging System equipped with a temperature controlled stage and Olympus cellSens Dimension 1.9 image acquisition software (Olympus). To image the ligand induced recruitment of ARRB2 to either AVPR2 or ADRB2, HeLa cells were transiently transfected with the expression constructs for ADRB2-11S and 114-ARRB2 or AVPR-114 and 11S-ARRB2 (500 ng DNA/sample for each construct) and plated in 35 mm dishes (Ibidi USA) in growth medium at a

density of 200,000 cells per dish. After 24 h of incubation, the cells were serum-starved in OptiMEMI for 4 h. Immediately prior to imaging, the medium was replaced with Opti-MEM supplemented with Nano-Glo® Live Cell substrate (10 μM final furimazine). Shortly after initiation of bioluminescence time-lapse imaging (for exposure times and gain settings see Supporting Figure s14), AVP (1 μM final concentration, AVPR/ARRB2 interaction) or isoproterenol (100 μM final concentration, ADRB2/ARRB2 interaction) were added (supplemented with Nano-Glo® Live Cell Substrate) by injection, and cells were continuously imaged for the indicated period of time. Image processing and analysis was performed using ImageJ v1.49[10] and GraphPad Prism 6, respectively.

SUPPORTING REFERENCES

[1] Ohana, R. F., Encell, L. P., Zhao, K., Simpson, D., Slater, M. R., Urh, M., and Wood, K. V. (2009) HaloTag7: a genetically engineered tag that enhances bacterial expression of soluble proteins and improves protein purification, *Protein Expr. Purif. 68*, 110-120.

[2] Los, G. V., Encell, L. P., McDougall, M. G., Hartzell, D. D., Karassina, N., Zimprich, C., Wood, M. G., Learish, R., Ohana, R. F., Urh, M., Simpson, D., Mendez, J., Zimmerman, K., Otto, P., Vidugiris, G., Zhu, J., Darzins, A., Klaubert, D. H., Bulleit, R. F., and Wood, K. V. (2008) HaloTag: a novel protein labeling technology for cell imaging and protein analysis, *ACS Chem. Biol. 3*, 373-382.

[3] Encell, L. P., Friedman Ohana, R., Zimmerman, K., Otto, P., Vidugiris, G., Wood, M. G., Los, G. V., McDougall, M. G., Zimprich, C., Karassina, N., Learish, R. D., Hurst, R., Hartnett, J., Wheeler, S., Stecha, P., English, J., Zhao, K., Mendez, J., Benink, H. A., Murphy, N., Daniels, D. L., Slater, M. R., Urh, M., Darzins, A., Klaubert, D. H., Bulleit, R. F., and Wood, K. V. (2012) Development of a dehalogenase-based protein fusion tag capable of rapid, selective and covalent attachment to customizable ligands, *Current chemical genomics 6*, 55-71.

[4] Ohana, R. F., Hurst, R., Vidugiriene, J., Slater, M. R., Wood, K. V., and Urh, M. (2011) HaloTag-based purification of functional human kinases from mammalian cells, *Protein Expr. Purif. 76*, 154-164.

[5] Petrosino, J., Rudgers, G., Gilbert, H., and Palzkill, T. (1999) Contributions of aspartate 49 and phenylalanine 142 residues of a tight binding inhibitory protein of beta-lactamases, *J. Biol. Chem. 274*, 2394-2400.

[6] Horton, R. M., Hunt, H. D., Ho, S. N., Pullen, J. K., and Pease, L. R. (1989) Engineering hybrid genes without the use of restriction enzymes: gene splicing by overlap extension, *Gene 77*, 61-68.

[7] Swanson, B., Fan, F., Wood, K.V. (2007) Enhanced response dynamics for transcription analysis using new pGL4 luciferase reporter vectors, *Cell Notes 17*, 3-5.

[8] Slater, M., Hartzell, D., Hartnett, J., Wheeler, S., Stecha, P., and Karassina, N. (2008) Achieve the protein expression level you need with the mammalian HaloTag® 7 Flexi® vectors, *Promega Notes 100*, 16-18.

[9] Hall, M. P., Unch, J., Binkowski, B. F., Valley, M. P., Butler, B. L., Wood, M. G., Otto, P., Zimmerman, K., Vidugiris, G., Machleidt, T., Robers, M. B., Benink, H. A., Eggers, C. T., Slater, M. R., Meisenheimer, P. L., Klaubert, D. H., Fan, F., Encell, L. P., and Wood, K. V. (2012) Engineered luciferase reporter from a deep sea shrimp utilizing a novel imidazopyrazinone substrate, *ACS Chem. Biol. 7*, 1848-1857.

[10] Schneider, C. A., Rasband, W. S., and Eliceiri, K. W. (2012) NIH Image to ImageJ: 25 years of image analysis, *Nat. Methods 9*, 671-675.